Magnetic Ordering in the Rare Earth Iron Germanates $HoFeGe_2O_7$ and $ErFeGe_2O_7$

C. Cascales,*,† E. Gutiérrez Puebla,† S. Klimin,‡ B. Lebech,§ A. Monge,† and M. N. Popova‡

Instituto de Ciencia de Materiales de Madrid, CSIC, Cantoblanco, E-28049 Madrid, Spain, Institute of Spectroscopy, Russian Academy of Sciences, 142092 Troitsk, Moscow region, Russian Federation, and Condensed Matter Physics and Chemistry Department, Risø National Laboratory, DK-4000 Roskilde, Denmark

Received April 21, 1999. Revised Manuscript Received June 14, 1999

$RFeGe_2O_7$ (R = Ho, Er) have been prepared in polycrystalline form, and their crystal structures have been refined from room-temperature high-resolution neutron diffraction data by the Rietveld method. Both materials are isostructural, space group $P2_1/m$ (no. 11), $Z = 4$. The most interesting feature of the structure is the existence of flattened chains of RO_7 polyhedra along the *b* axis, which linked in the *c* direction through pairs of FeO_6 octahedra form layers parallel to the *bc* crystal plane. Magnetic susceptibility measurements between 350 and 1.7 K reveal the existence of two anomalies for both compounds, at T_1 and T_2, ($T_2 < T_1$), 39 and 12 K, 40 and 8 K, for R = Ho and Er, respectively. From low-temperature neutron diffraction data, three-dimensional antiferromagnetic ordering in both compounds is established, with a simultaneous setting up of the order for R^{3+} and Fe^{3+} sublattices at $T_N = T_1$. The propagation vector of the magnetic structure is $k = [0, 0, 0]$. In each case the magnetic structure consists of a ferromagnetic arrangement of all R^{3+} and Fe^{3+} magnetic moments within one *ac* plane, whereas the corresponding moments in up and down adjacent planes are oppositely aligned, leading to 3D AF coupling along the *b* direction. Kramers doublets splittings in the region of the $^4I_{15/2} \rightarrow {}^4I_{13/2}$ optical transitions of the Er compound have been observed in high-resolution optical absorption spectra. From these spectral measurements the temperature found for the magnetic ordering coincides with that T_N determined by neutron diffraction data. Moreover optical data also show that T_2 in $\chi_m(T)$ does not correspond to any phase transition but it is most probably caused by the population changes within the ground Er^{3+} Kramers doublet split by the exchange interaction with the ordered Fe^{3+} subsystem.

Introduction

The crystal structure of the family of germanates $RMGe_2O_7$, in which M and R represent trivalent metals Al or Ga and rare earth ions from La to Dy, respectively, was found in the 1980s[1,2] to be a monoclinic $NdAlGe_2O_7$ structure type, space group $P2_1/c$. Some studies of luminescence and stimulated emission were carried out for Nd^{3+}-containing compounds.[2] In the family with M = Fe, and depending on the size of R, the phase formation corresponds to the mentioned[1,3−4] monoclinic type for the larger R cations, i.e., from La to Gd, and to another one,[5] very recently described by some of the authors[6] for the smaller (Y and Tb to Yb) rare earths. This last $YFeGe_2O_7$ structure type is also monoclinic, space group $P2_1/m$ (no. 11), $Z = 4$, with flattened chains of RO_7 polyhedra running along the *b* axis, which linked in the *c* direction through pairs of FeO_6 octahedra form layers parallel to the *bc* crystal plane. Magnetization[5−7] and Mössbauer[5] measurements between 350 and 1.7 K reveal one peak at 38 K for R = Y and the existence of two anomalies, at T_1 and T_2 ($T_2 < T_1$) for the 4f-containing compounds. Before the current knowledge of this structure, two alternative models[5] were initially proposed to explain these two characteristic maxima. Recently, from low-temperature neutron powder diffraction NPD data on $TbFeGe_2O_7$, three-dimensional antiferromagnetic ordering was established,[6] both Fe and Tb sublattices getting simultaneously ordered at $T_N = 42$ K. This temperature coincides with the observed for the susceptibility peak at T_1. The magnetic

* To whom correspondence should be addressed. Fax: 34 91 3720623. E-mail: immcc53@fresno.csic.es.
† Instituto de Ciencia de Materiales de Madrid.
‡ Russian Academy of Sciences.
§ Risø National Laboratory.

(1) Jarchow, K.; Klaska, K. H., Schenk-Strauss, H. *Z. Krystallogr.* **1985**, *172*, 159.
(2) Kaminskii, A. A.; Mill, B. V.; Butashin, A. V.; Belokoneva E. L.; Kurbanov, K. *Phys. Status Solidi A* **1987**, *103*, 575.
(3) Mill, B. V.; Kazei, S. A.; Reiman, S. Y.; Tamazyan, S. A.; Khamdamov F. D.; Bykova, L. Yu. *Vestn. Mosk. Gos. University Fiz. Astron.* **1987**, *28*, 95.
(4) Bucio, L.; Cascales, C.; Alonso, J. A.; Rasines, I. *J. Phys.: Condens. Matter* **1996**, *8*, 2641.
(5) Kazei, Z. A.; Kuyanov, Z. A., Levitin, R. Z.; Markosyan, A. S.; Mill, B. V.; Reiman, S. Y.; Snegirev V. V.; Tamazyan, S. A. *Sov. Phys. Solid State* **1989**, *31*, 233.
(6) Cascales, C.; Bucio, L.; Gutiérrez Puebla, E.; Rasines, I.; Fernández Díaz, M. T. *Phys. Rev. B* **1998**, *57*, 5240.
(7) Cascales, C.; Bucio, L.; Gutiérrez Puebla, E.; Rasines, I.; Fernández Díaz, M. T. *J. Alloys Compd.* **1998**, *275−277*, 29.

10.1021/cm991053m CCC: $18.00
Published on Web 08/11/1999

moments are ferromagnetically coupled within each *ac* plane, while the moments in up and down adjacent perpendicular to *b* planes are oppositely aligned.

The aim of this article is to characterize the microscopic magnetic behavior of $RFeGe_2O_7$, R = Ho and Er, comparing it with the isomorphous $TbFeGe_2O_7$. In this way the synthesis of these compounds, the refinement of their crystal structures, as well as low-temperature neutron diffraction studies were undertaken in order to investigate the nature of the anomalies displayed by the magnetic measurements and to establish the magnetic structure of the low temperature ordered phases. The use of high-resolution optical spectroscopy of $ErFeGe_2O_7$ enable the determination of the temperature dependence of the spectral line splittings and shifts, providing an alternative and complementary deep insight in the study of the magnetic phase transition of this system.

Experimental Section

Preparation of the Samples. $RFeGe_2O_7$ (R = Ho, Er) were prepared as polycrystalline powder materials by solid-state reaction from analytical grade mixture of the stoichiometric required amounts of Fe_3O_4, GeO_2, and R_2O_3, with a slight excess of the Ge oxide to counteract their losses especially as a vitrified product. Samples were ground and heated in air to final temperatures of 1200 and 1250 °C, higher for the heavier R compound, for 2 weeks with intermediate regrinding. Standard X-ray powder diffraction analysis indicated that final samples were well crystallized and appeared, to the limit of the technique, free of other crystalline phases.

Crystal and Magnetic Structure Refinements. Neutron scattering experiments were performed on the TAS3 spectrometer at the DR3 nuclear reactor, Risø National Laboratory, which is operated by means of TASCOM, Triple Axis Spectrometer Command System. About 8 g of sample were used in both cases, contained in a cylindrical vanadium can and held in a liquid helium cryostat. Extensive and accurate data were obtained from diffraction patterns collected using a wavelength of 1.540 Å, in the large angular range $5° \leq 2\theta \leq 110.776°$, in steps of 0.0529°, at several temperatures between room temperature and 1.7 K. A full pattern was recorded in 6 h.

The Rietveld method was used to refine the crystal and magnetic structures. All the data were analyzed with the program FULLPROF.[8] A pseudo-Voigt function was chosen to generate the line shape of the diffraction peaks. The background was fitted to a polynomial refinable function. The low-temperature TAS3 patterns were refined, taking as starting parameters for each pattern those resulting from the refinement of the preceding one at higher temperature. In all cases the shifts in the atomic parameters on the final refinement cycle were zero up to the third decimal place.

Magnetic Measurements. A SQUID magnetometer (Quantum Design) operating from 350 to 1.7 K at 5000 Oe was used to carry out dc magnetic susceptibility measurements. Magnetization measurements were performed up to 90 kOe. Diamagnetic corrections[9] for the magnetic susceptibilities were taken into account.

Spectroscopic Measurements. Powder samples of $ErFeGe_2O_7$ were carefully ground, mixed with ethanol, and applied on a quartz platelet, which was inserted just before the InSb detector. The whole assembly was inside an optical cryostat in helium vapor. The temperature was measured by the Cu−Fe−Cu thermocouple, and was controlled within ±0.2 K in the range of temperatures between 130 and 4.2 K. The optical spectra of diffuse transmittance in the region of the $^4I_{15/2} \rightarrow {}^4I_{13/2}$ transition for the Er^{3+} ion were recorded by a high resolution (0.004 cm^{-1}) BOMEM DA3.002 Fourier transform spectrometer. Further details on the technique can be found in references.[10,11]

Crystal Structure of $RFeGe_2O_7$, R = Ho, Er

The $YFeGe_2O_7$ structure type, where Y can be substituted by a smaller rare earth, typically Tb to Yb, has been described for the Tb compound in a previous work.[6] It is monoclinic, space group $P2_1/m$ (no. 11), $Z = 4$, and contains three kinds of coordination polyhedra: distorted FeO_6 octahedra joined in pairs by edge sharing, RO_7 capped octahedra, the R−O distances all being of slightly different lengths, and four kinds of Ge atoms exhibiting the usual tetrahedral coordination, which are associated by sharing corners forming isolated Ge(1)-Ge(2)O_7 and Ge(3)Ge(4)O_7 diorthogroups. Its most interesting feature is the existence of flattened chains of RO_7 polyhedra along the *b* axis, which linked in the *c* direction through pairs of FeO_6 octahedra with which they share edges, form layers running parallel to the *bc* crystal plane. Ge_2O_7 diorthogroups are not connected neither in the *a* nor in the *b* directions, but they play a bridging role between parallel RO_7- and FeO_6-containing layers. Figure 1 illustrates a complete view of the structure. Further details on this structure type are described in the above mentioned reference.[6]

Table 1 includes the structural parameters for both Ho and Er compounds, obtained from NPD data at room temperature. A little amount (<2%) of Fe_2O_3 was detected in both prepared samples, and thus introduced as a secondary phase in the structural refinements. Figure 2 shows the observed and calculated profiles for $HoFeGe_2O_7$. The final refined positional and thermal parameters for both germanates are given in Table 2, and Table 3 consists of the main interatomic distances, including the intermetallic ones, in the *b* and *c* directions.

Magnetic Susceptibility Measurements

Figures 3 and 4 show the variation with temperature of the molar magnetic susceptibility χ_m for $RFeGe_2O_7$, R = Ho, Er. Whereas for the first compound a clear maximum is observed at 16 K, only a small anomaly is detected at 8 K for $ErFeGe_2O_7$. A more detailed analysis of these data reveals, for each compound, the presence of two different maxima in the thermal evolution of χ_m, as can be seen in $d(\chi_m T)$ vs T plots, at T_1 and T_2 ($T_2 < T_1$), 39 and 12 K, 40 and 8 K, the more intense appearing at T_2, for R = Ho and Er, respectively. These peaks could be related to transitions to antiferromagnetically ordered states of the Fe^{3+} and R^{3+} magnetic sublattices.

Figures 5 and 6 show the magnetization curves for $HoFeGe_2O_7$ and $ErFeGe_2O_7$ at various temperatures.

(8) Rodríguez Carvajal, J. FULLPROF *Program for Rietveld Refinement and Pattern Matching Analysis*; Abstracts of the Satellite Meeting on Powder Diffraction of the XVth Congress of the International Union of Crystallography, Toulouse, France, 1990; p 127. The program is a strongly modified version of that described by Wiles D. B.; Joung, R. A. *J. Appl. Crystallogr.* **1981**, *14*, 149.

(9) Boudreaux E. A.; Mulay, L. N. *Theory and Applications of Molecular Paramagnetism*; Wiley: New York, 1976; pp 494−5.

(10) Popova, M. N. *10th Feofilov Symposium on Spectroscopy of Crystals Activated by Rare Earth and Transition Metal Ions*; Ryskin; A. I., Masterov, V. F., Eds. *SPIE* **1996**, *2706*, 182.

(11) Chepurko, G. G.; Kazei, Z. A.; Kudrjavtsev, D. A.; Levitin, R. Z.; Mill, B. V.; Popova, M. N.; Snegirev, V. V. *Phys. Lett. A* **1991**, *157*, 81.

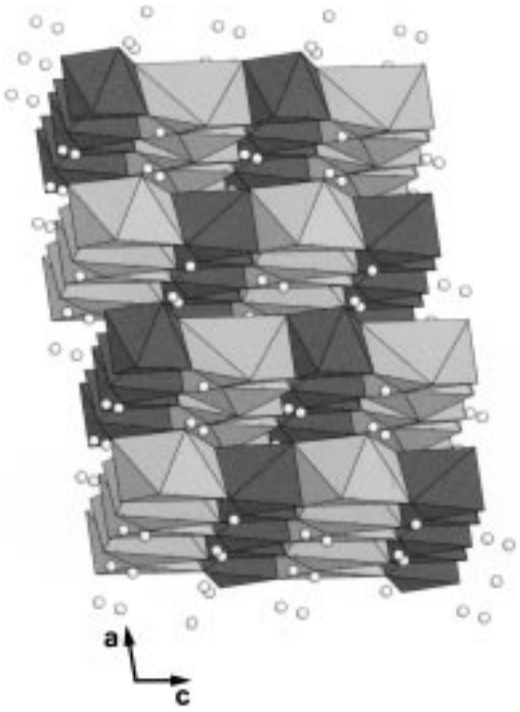

Figure 1. Complete view of the $RFeGe_2O_7$ structure type showing the parallel layers resulting from the association in the *bc* plane of chains of RO_7 capped octahedra (light gray polyhedra) and isolated pairs of edge-sharing FeO_6 octahedra (dark gray polyhedra). These layers are linked through Ge_2O_7 diorthogroups, represented only as small spheres between them.

Table 1. Lattice Parameters and Discrepancy Factors for $RFeGe_2O_7$, R = Ho, Er, *S. G.* $P2_1/m$ (No. 11), $Z = 4$[a]

	Ho		Er	
lattice parameters				
a (Å)	9.6359(9)[b]	9.6273(11)[c]	9.6413(11)[b]	9.6397(15)[c]
b (Å)	8.4758(8)	8.4649(10)	8.5100(9)	8.5086(12)
c (Å)	6.6709(7)	6.6722(9)	6.6501(8)	6.6517(11)
β (deg)	100.610(7)	100.57(1)	100.833(9)	100.81(1)
V (Å^3)	535.5(1)	534.5(3)	535.9(3)	535.8(3)
no. reflections	804[d]	1371[e]	745[d]	1376[e]
reliability factors (%)				
χ^2	1.81	3.90	1.89	3.36
R_p	7.42	10.0	8.18	10.6
R_{exp}	7.03	6.92	7.67	7.59
R_{Bragg}	7.46	7.76	8.90	9.67
R_f	4.48	4.14	4.87	5.11
R_{mag}	-	8.90	-	10.2

[a] From NPD (TAS3) data. [b] Room temperature. [c] 1.7 K. [d] Nuclear cell. [e] Magnetic cell.

For both compounds, at temperatures above 30 K, the magnetization vary almost linearly with the field. When the temperature descends, it is seen that the isotherms begin to display a sharp increase in the magnetization, which correspond to a metamagnetic transition. The discontinuity in the magnetization curve, or better, the maximum in the differential susceptibility dM/dH vs H indicates fields of ~24 800 and 28 700 Oe, for R = Ho and Er, respectively, for this transition.

At temperatures up ~60 K to room temperature, a Curie−Weiss behavior is observed in both cases, $\chi_m^{-1} = 1.628(2) + 0.06233(8)$ T mol emu^{-1} ($r = 0.9996$), and $1.374(6) + 0.08167(3)$ T mol emu^{-1} ($r = 0.99997$), with paramagnetic Curie temperatures $\theta_c = -26.12(3)$ and $-16.8(1)$ K, and effective magnetic moments $\mu_{eff} = 11.4$-

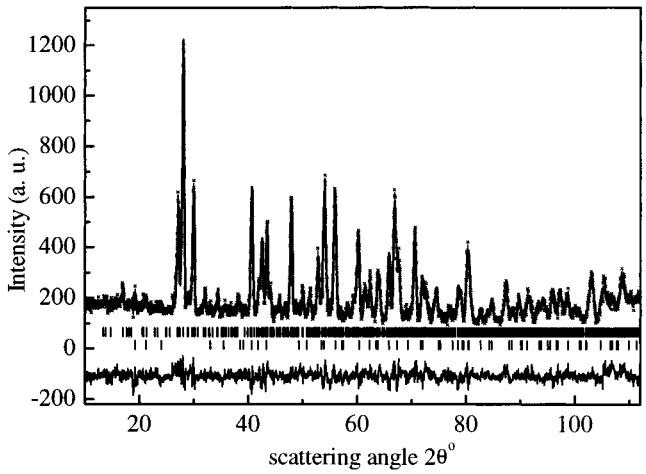

Figure 2. Observed, calculated, and difference neutron diffraction (DR3 TAS3 Risø NL) profiles of $HoFeGe_2O_7$ at room temperature. Vertical marks correspond to the position of the allowed Bragg reflections for the crystallographic structure. Second row of vertical marks corresponds to the impurity of Fe_2O_3.

Table 2. Final Refined Positional and Thermal Parameters for $RFeGe_2O_7$, R = Ho, Er, at Room Temperature

	x/a	y/b	z/c	B (Å^2)[a]
Ho	0.749(2)	0.544(1)	0.761(3)	0.02(2)
Ge(1)	0.527(2)	0.75	0.050(4)	0.03(1)
Ge(2)	0.553(3)	0.25	0.475(4)	0.03(1)
Ge(3)	0.953(3)	0.25	0.021(4)	0.03(1)
Ge(4)	0.030(2)	0.25	0.550(3)	0.03(1)
Fe(1)	0.765(2)	0.454(1)	0.264(2)	0.09(2)
O(1)	0.639(2)	0.421(2)	0.457(3)	0.24(1)
O(2)	0.871(3)	0.25	0.338(4)	0.24(1)
O(3)	0.939(3)	0.25	0.765(5)	0.24(1)
O(4)	0.572(3)	0.25	0.771(4)	0.24(1)
O(5)	0.857(2)	0.059(2)	0.012(3)	0.24(1)
O(6)	0.140(3)	0.25	0.146(5)	0.24(1)
O(7)	0.137(2)	0.090(3)	0.526(3)	0.24(1)
O(8)	0.388(3)	0.25	0.344(5)	0.24(1)
O(9)	0.597(3)	0.25	0.151(4)	0.24(1)
O(10)	0.640(2)	0.582(2)	0.062(3)	0.24(1)
Er	0.749(3)	0.554(1)	0.756(5)	0.01(3)
Ge(1)	0.532(3)	0.75	0.052(5)	0.06(1)
Ge(2)	0.561(3)	0.25	0.473(4)	0.06(1)
Ge(3)	0.953(3)	0.25	0.025(4)	0.06(1)
Ge(4)	0.018(3)	0.25	0.561(5)	0.06(1)
Fe(1)	0.756(3)	0.454(1)	0.256(4)	0.05(2)
O(1)	0.633(3)	0.445(2)	0.451(4)	0.23(1)
O(2)	0.881(4)	0.25	0.358(6)	0.23(1)
O(3)	0.954(3)	0.25	0.753(6)	0.23(1)
O(4)	0.582(3)	0.25	0.751(6)	0.23(1)
O(5)	0.858(2)	0.102(2)	0.013(3)	0.23(1)
O(6)	0.137(4)	0.25	0.151(6)	0.23(1)
O(7)	0.144(3)	0.095(3)	0.536(5)	0.23(1)
O(8)	0.397(3)	0.25	0.374(5)	0.23(1)
O(9)	0.622(4)	0.25	0.170(6)	0.23(1)
O(10)	0.641(3)	0.581(31)	0.054(4)	0.23(1)

[a] Isotropic thermal parameters have been constrained on the same value for each type of atom.

(2) and 9.9(2) MB, for Ho and Er compounds respectively, close to expected values, 12.1 and 11.3 MB, considering free ion magnetic moments for R^{3+} and high-spin Fe^{3+} cations.

Magnetic Ordering and Group Theory Analysis in $RFeGe_2O_7$

The low-temperature NPD patterns for the title germanates, in a range of the 2θ scattering angle from

Table 3. Main Interatomic Distances (Å) in $RFeGe_2O_7$, R = Ho, Er

	Ho	Er		Ho	Er
R−O(1)	2.36(3)	2.32(4)	Ge(2)−O(1) ×2	1.67(2)	1.82(2)
R−O(4)	3.03(2)	3.04(3)	Ge(2)−O(4)	1.95(4)	1.82(5)
R−O(5)	2.00(3)	2.26(3)	Ge(2)−O(8)	1.67(4)	1.59(4)
R−O(6)	2.08(2)	2.03(3)			
R−O(7)	2.40(3)	2.39(4)	Ge(3)−O(3)	1.69(2)	1.81(5)
R−O(8)	2.22(2)	2.25(3)	Ge(3)−O(5) ×2	1.86(2)	1.56(3)
R−O(10)	2.45(3)	2.42(4)	Ge(3)−O(6)	1.84(4)	1.82(5)
Fe−O(1)	1.96(3)	1.90(4)	Ge(4)−O(2)	1.88(4)	1.71(5)
Fe−O(2)	2.03(2)	2.15(3)	Ge(4)−O(3)	1.81(4)	1.52(5)
Fe−O(5)	2.05(3)	2.12(3)	Ge(4)−O(7) ×2	1.73(3)	1.82(3)
Fe−O(7)	1.93(2)	1.93(4)			
Fe−O(9)	2.39(2)	2.18(3)	R−R, *b*	3.49(1)	3.34(2)
Fe−O(10)	1.96(3)	1.92(4)		4.99(1)	5.17(2)
			Fe−Fe, *b*	3.45(1)	3.48(1)
Ge(1)−O(4)	1.66(4)	1.86(4)		5.02(1)	5.03(1)
Ge(1)−O(9)	1.63(4)	1.89(5)	R−Fe, *c*	3.45(2)	3.42(4)
Ge(1)−O(10) ×2	1.78(2)	1.78(3)		3.44(2)	3.44(4)

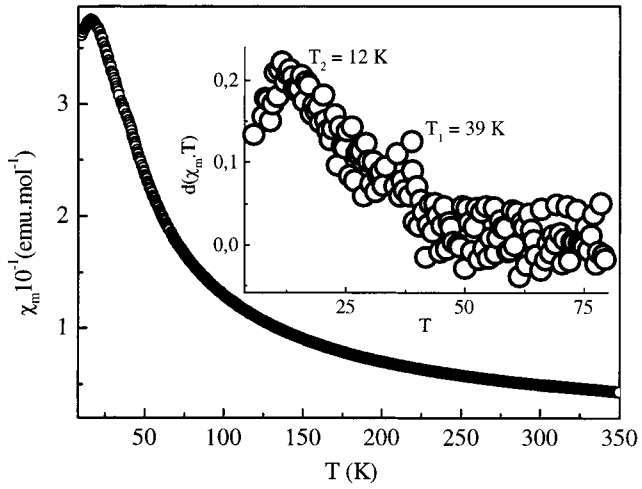

Figure 3. Molar magnetic susceptibility $\chi_m(T)$ for $HoFeGe_2O_7$. The inset shows the dependence of the derivative with respect to the temperature of the product $\chi_m T$.

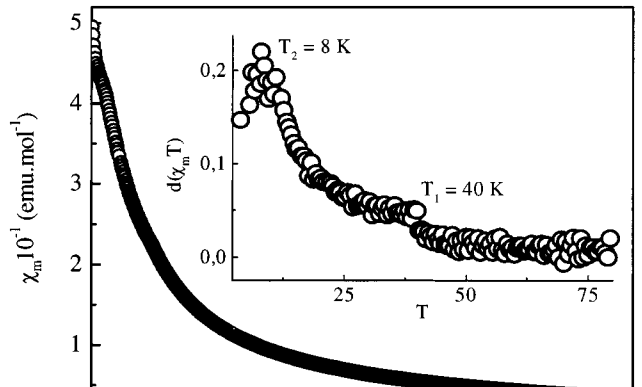

Figure 4. Molar magnetic susceptibility $\chi_m(T)$ for $ErFeGe_2O_7$. The inset shows the dependence of the derivative with respect to the temperature of the product $\chi_m T$.

5° to 111°, show a series of extra peaks appearing below 40 K, which correspond to the three-dimensional antiferromagnetic ordering of Fe^{3+} and R^{3+} subcells. The intensities of the magnetic reflections grow regularly to reach the maximum at 1.7 K, this maximun being more intense for the Ho compound.

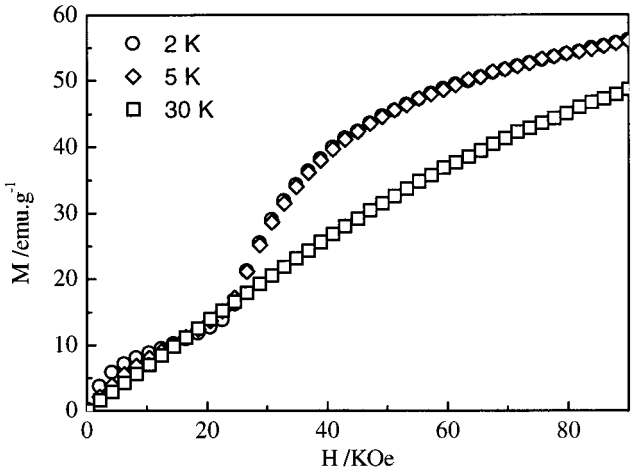

Figure 5. Isotherms of the magnetization for $HoFeGe_2O_7$.

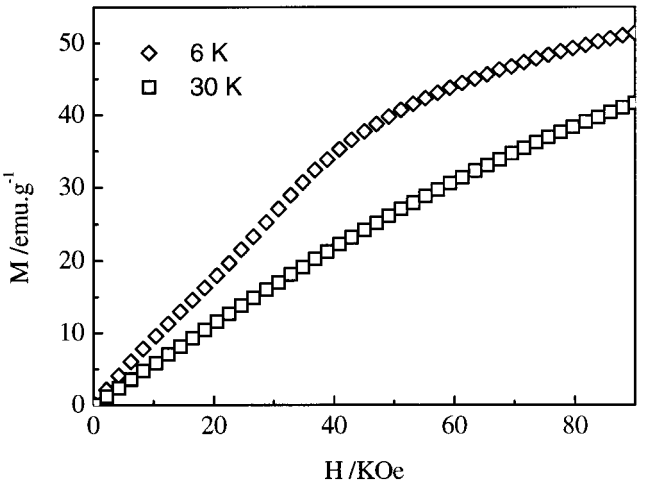

Figure 6. Isotherms of the magnetization for $ErFeGe_2O_7$.

Below 40 K, all the observed Bragg peaks were indexed within a commensurate lattice with approximately the same unit cell parameters of the crystallographic one. Since "pure magnetic" reflections are those indexed $0k0$ (being $0\ k\ 0$, $k = 2n + 1$, an extinction condition of $P2_1/m$), some ordering of the magnetic moments perpendicular to the *b* axis can be though, a supposition which can be acceptably justified by the expression of the intensity of the nonpolarized neutron beam diffracted by a powdered sample.

The chemical unit cell contains four R^{3+} (Ho or Er) and four Fe^{3+} atoms. Since the lattice is primitive, the magnetic structure can be described by considering the magnetic moments of one R and one Fe atoms, and the remaining magnetic moments can be deduced by means of the t_N Bravais translation vector, according to $m_{j_N} = m_{j_o} e^{-2\pi i k t_N}$. Because the magnetic and chemical unit cells are identical, this ordered magnetic structure can be described in terms of a $k = [0,0,0]$ propagation vector.

From the group-theory analysis and following the method previously described,[6,12] which studies the possible magnetic structures compatible with the crystal symmetry, all possible forms of ordering of the magnetic moments are determined through the base functions of the irreducible representations of the wave vector group G_k, which contains only those symmetry operations of

(12) Bertaut, E. F. *Acta Crystallogr. A* **1968**, *24*, 217.

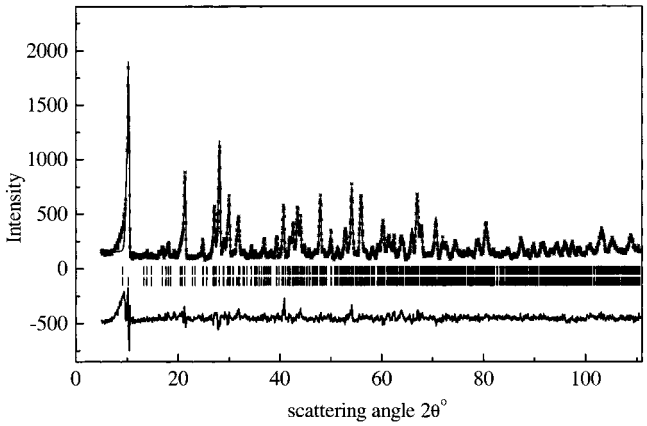

Figure 7. Neutron diffraction pattern of $HoFeGe_2O_7$ at 1.7 K. The solid line is the calculated profile and vertical marks correspond to the position of the Bragg reflections for the crystallographic (first row) and magnetic (second row) structures. The difference curve is plotted at the bottom of the figure.

the high-temperature space group ($T > T_N$) which keeps invariant the propagation vector or transforms it into an equivalent vector.

The irreducible representations contained in Γ (R^{3+}) and Γ (Fe^{3+}) are, in both cases, $A_g + 2B_g$. And because only vectors belonging to the same representation of both sites (R and Fe) may be coupled,[12] in first approximation, two possibilities for the ordering of the magnetic moments of both R and Fe subcells can be considered. For Γ^1 (A_g) the magnetic moments have a single component along the *b* axis, whereas for Γ^2 (B_g) the moment is described by the *x* and *z* components, in the *ac* plane.

Magnetic Structure Refinements

The situation represented by the first A_g representation must be discarded because as previously indicated it does not correspond to the experimental data. B_g, which considers the R^{3+} and Fe^{3+} magnetic moments restricted to the *ac* plane, offers two possibilities of coupling between these atoms: the antiferromagnetic or the ferromagnetic mode, $A_x = m_{xFe} - m_{xR}$, $A_z = m_{zFe} - m_{zR}$, and $F_x = m_{xFe} + m_{xR}$, $F_z = m_{zFe} + m_{zR}$, respectively. The best fit of the experimental data at 1.7 K is obtained for the B_g representation, these data being favorably explained by the ferromagnetic coupling between the magnetic moments of Fe^{3+} and R^{3+} in the *ac* planes.

For the analysis of the low-temperature NPD data of both compounds, a refinement of the pattern for every temperature was performed. In each case, the crystal structure was refined taking as starting parameters those obtained for the data collected at room temperature. The magnetic structure was refined as an independent phase for which only magnetic atoms were defined. The scale and thermal factors were constrained for both chemical and magnetic structures. Moreover, in the starting step of the analysis of NPD data by the Rietveld method, the magnetic moments were considered as aligned along the *c* axis.

In Figure 7, the observed and calculated patterns at 1.7 K for $HoFeGe_2O_7$ are represented. Tables 1 and 4 show a summary of the refined structural parameters and magnetic moments at this temperature, respectively. The magnetic moments are written in the Cartesian components allowed by the magnetic structure (S_x, 0, S_z) as well as in spherical coordinates. The magnetic structure of both $RFeGe_2O_7$ materials consists of a ferromagnetic arrangement of all Fe^{3+} and R^{3+} magnetic moments, whose directions form angles with *c* axis (*positive* direction), as indicated in Table 4, within one *ac* plane, whereas the moments in the up and down adjacent *ac* planes are oppositely aligned, leading then to 3D antiferromagnetic coupling along the *b* direction. Figure 8a shows a schematic view of the disposition of magnetic moments for both Ho and Er compounds on the *ac* plane. Figure 8b is the projection of the magnetic structure onto *bc* planes.

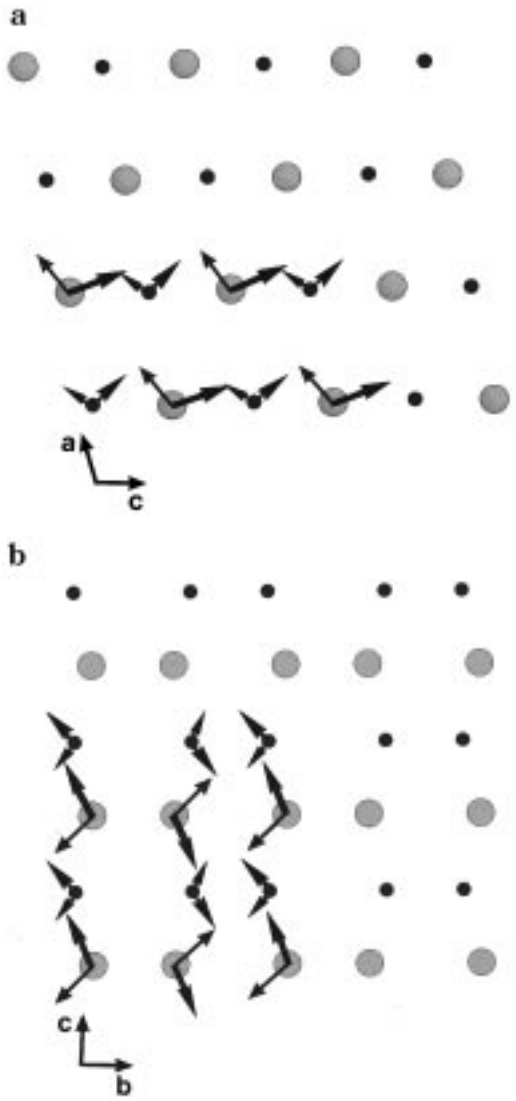

Figure 8. Projection of the magnetic structure onto (a) *ac* planes and (b) *bc* planes, small and large spheres are representing Fe and R atoms, thick and thin arrows correspond to Ho and Er compounds, respectively.

Table 4. Magnetic Moments for Fe^{3+} and R^{3+} in $RFeGe_2O_7$ at 1.7 K, in Cartesian and Spherical Coordinates

	R = Ho				R = Er			
	S_x (μ_B)	S_z (μ_B)	M (μ_B)	θ (deg)	S_x (μ_B)	S_z (μ_B)	M (μ_B)	θ (deg)
Fe^{3+}	2.3(2)	3.3(1)	3.7(1)	38.8	1.6(2)	2.9(3)	3.5(2)	153.6
R^{3+}	2.5(2)	6.8(1)	6.8(1)	20.8	4.1(2)	3.3(2)	5.7(2)	135.2

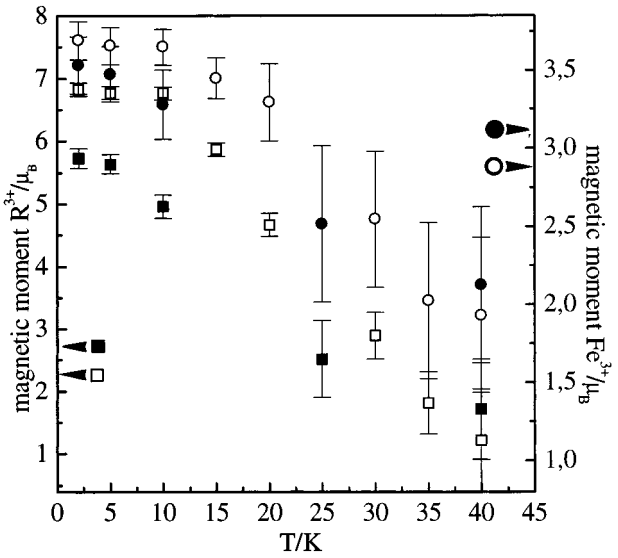

Figure 9. Thermal evolution of the ordered magnetic moments in $FeRGe_2O_7$, circles and squares represent Fe^{3+} and R^{3+}, open and solid figures corresponding to Ho and Er compounds, respectively.

It is interesting to compare these results with those obtained for the isomorphous $TbFeGe_2O_7$ compound.[6] The magnetic structure of the three compounds is the same, but whereas for both Tb and Ho materials the magnetic moments of the parallel to *c*, $-RO_7-FeO_6-RO_7-$ chains can be viewed as nearly aligned (more in the Tb case) along the positive direction of the *c* axis, for $ErFeGe_2O_7$ the moments are turned in the opposite direction, and thus the magnetic moments of Er^{3+} may be regarded as closer to the *a* than to the *c* axis.

The thermal variation of Fe^{3+} and R^{3+} magnetic moments is represented in Figure 9, where it is depicted that 3D magnetic order begins to develop at the same temperature, below 40 K, in both sublattices for each compound, the important error bars being due to the small ordered moments of Fe^{3+} when its ordering is not completely reached. The magnetic moment of Ho^{3+} attains its saturation value, 6.8(1) μ_B, below 10 K, whereas a lower temperature, about 5 K, is required for that of Er^{3+}, 5.7(2) μ_B.

High-Resolution Spectroscopic Measurements

A crystal field of any symmetry lower than cubic lifts all but Kramers degeneracy of the levels of a free rare earth ion with odd number of electrons. Kramers doublets are further split only by a external magnetic field or by the magnetic field that originates during the magnetic ordering of a system. The spectral line of an optical transition in this case splits into four components, Figure 10. The detection of the splitting and narrowing of spectral lines during the magnetic ordering of a system constitutes the basis of the spectral method for studying the magnetic phases transitions. Thus the Er^{3+} Kramers ion (intrinsic or introduced as a dopant) can be considered as a spectroscopic probe in the study of magnetic interactions in the current $RFeGe_2O_7$ structure.

For the paramagnetic phase, i.e., above 40 K, seven lines corresponding to optical transitions from the ground state to crystal field levels of the $^4I_{13/2}$ multiplet

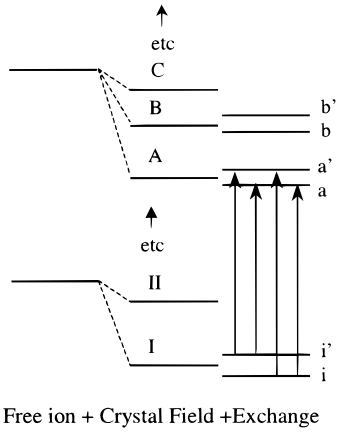

Figure 10. Levels of a Kramers ion in a magnetically ordered system.

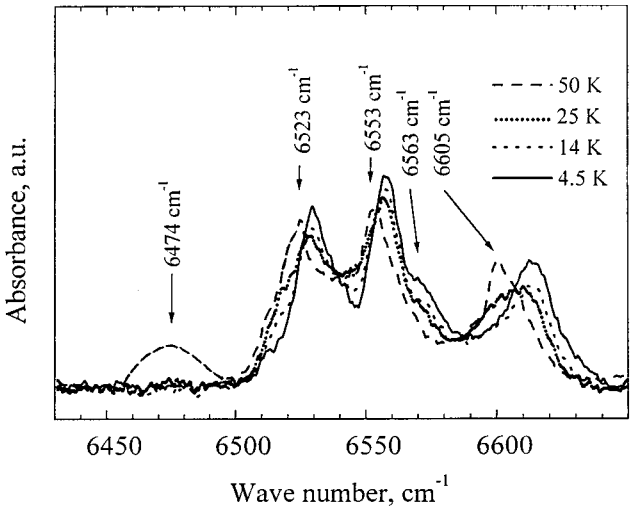

Figure 11. Low-frequency part of the $^4I_{15/2} \rightarrow {}^4I_{13/2}$ transition of Er^{3+} in $ErFeGe_2O_7$ at different temperatures.

Table 5. Energies (cm^{-1}) of Some Measured Crystal Field Levels of Er^{3+} in $ErFeGe_2O_7$

$^4I_{15/2}$	0	53	90	115			
$^4I_{13/2}$	6523	6552	6563	6605	6719	6770	6837

are present in the absorbance spectra. According to the point symmetry of Er^{3+} in the cell, this number coincides with the number of expected Stark levels originated from the crystal field splitting of $^4I_{13/2}$. Thus, the existence of only one position for Er^{3+} in $RFeGe_2O_7$ is confirmed. Positions of crystal field levels of the $^4I_{13/2}$ multiplet are given in Table 5. Table 5 also list the first three excited levels of the $^4I_{15/2}$ ground multiplet as determined from the analysis of positions and temperature dependencies of spectral lines emerging due to the thermal population of these levels.

Figure 11 presents the lowest frequency spectral lines of the $^4I_{15/2} \rightarrow {}^4I_{13/2}$ transition at different temperatures between 50 K ($> T_N$) and 4.5 K ($< T_N$). The 6474 cm^{-1} line seen at 50 K originates from the transition from the first excited level at 53 cm^{-1} to the 6523 cm^{-1} level of $^4I_{13/2}$. A growing splitting of the 6523 cm^{-1} line accompanied by a diminishing intensity of the low frequency component, is clearly observed when the temperature descends from 40 to 4.5 K. Such a behavior points to the splitting of Kramers doublets of the Er^{3+} ion, caused by a magnetic ordering of the compound. The decrease of the intensity of the low-frequency

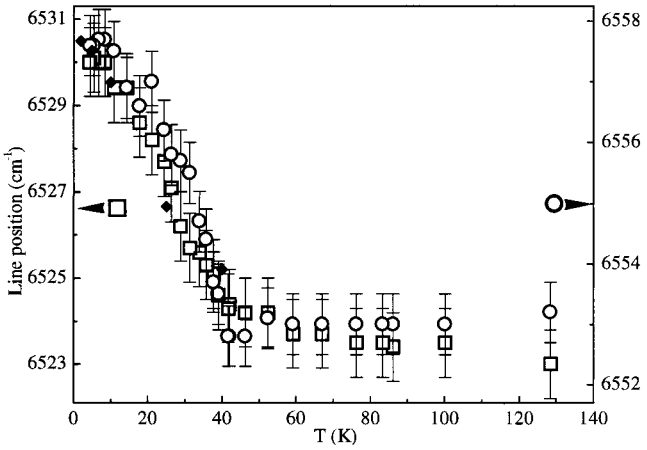

Figure 12. Temperature dependences of the positions of the two lowest lines of $^4I_{13/2}$. Diamonds are the magnetic moments of the iron subsystem, in arbitrary units, determined from NPD measurements.

component of the split line corresponds to the depopulation of the upper component of the ground Kramers doublet split by magnetic interactions in the ordered state; see Figure 11. Thus, there is a good spectroscopic evidence of magnetic ordering in $ErFeGe_2O_7$.

The splittings of spectral lines are comparable to their widths and so it is not possible to distinguish all components clearly. Instead we follow the shift of the strongest component of the split line, which is proportional to the splitting. Plots of the thermal dependence of the shifts, for the two lower frequency spectral lines of the $^4I_{15/2} \rightarrow {}^4I_{13/2}$ optical transition, 6523 and 6553 cm^{-1}, presented in Figure 12, reveal the temperature of 40 K corresponding to the points of inflection on curves, for the magnetic transition in $ErFeGe_2O_7$. Moreover the ground doublet splitting of Er^{3+} ion is proportional, within the experimental error, to the determined magnetic moments $\mu_{Fe}(T)$ of the iron subsystem (see Figure 12), and hence the Fe−Er interaction gives the main contribution to the splitting. Consequently, the Er^{3+} ground-state splitting can be considered in the same way as a Zeeman splitting in the magnetic field created by the ordered iron subsystem, and a molecular field approach will be valid.[11]

On the other hand, the spectral shapes are identical at 14 and 4.5 K, which means that there is no magnetic transition between these temperatures. We think that the origin of the observed maximum at 8 K in the thermal evolution of the magnetic susceptibility lies in the depopulation of the upper component of the ground Er^{3+} Kramers doublet split by the magnetic interactions.[11] Indeed the first excited state in the $^4I_{15/2}$ ground manifold of $ErFeGe_2O_7$ lies sufficiently high, 53 cm^{-1}, and in a first approximation only the ground doublet can be considered to contribute to the magnetic moment of the erbium subsystem. Estimations made in the framework of the molecular field approach show[11] that changes of population within two components of a doublet separated by Δ result in a magnetic susceptibility peak at $kT_p = \Delta/1.53$, where k is the Boltzmann constant. Thus, the observed magnetic susceptibility maximum at 8 K reveals $\Delta = 8.5\ cm^{-1}$, which agree very reasonably with the observed spectral line splittings.

Conclusions

In $RFeGe_2O_7$ (R = Tb, Ho or Er), 3D order for both magnetic sublattices starts simultaneously at $T_N \sim 40$ K, and thus only one irreducible representation is favored in the transition. For $ErFeGe_2O_7$, T_N found from low-temperature NPD data coincides very satisfactory with the temperature of the magnetic ordering determined from spectroscopic data. Furthermore, the analysis of the NPD data indicates that no magnetic phase transition or spin reorientation occurs at the most important maximum, T_2, in the $\chi_m(T)$ curves, this fact being confirmed in $ErFeGe_2O_7$ by spectral measurements in the region of the $^4I_{15/2} \rightarrow {}^4I_{13/2}$ optical transition of Er^{3+}. The $\chi_m(T_2)$ maximum is probably caused by population changes within the ground Er^{3+} Kramers doublet, split by the exchange interaction with the ordered iron subsystem. These splittings were found to be proportional to the determined from NPD magnetic moments $\mu_{Fe}(T)$. It follows from this fact that the Fe−Er interactions are stronger than the Er−Er ones.

Fe−R interactions on $RFeGe_2O_7$ compounds are highly anisotropic, reflecting the different direction of the anisotropy of the corresponding rare earth. Consequently, although possessing the same structure of magnetic moments in a ordered state, which is described by the same B_g irreducible representation, for the Ho material the magnetic moments of the parallel to c $-HoO_7-FeO_6-HoO_7-$ chains can be viewed as aligned along the positive direction of the c axis, whereas Er moments on $FerGe_2O_7$ are regarded as closer to a than to c axis.

Acknowledgment. The authors acknowledge the financial support of the DGESIC of Spain, under project PB97-1200, and of the Russian Foundation for Basic Research (grant 98-02-17620). The neutron scattering experiments reported in this paper were performed at the DR3 reactor at Risø National Laboratory and supported by the Commission of the European Community through the Training and Mobility of Researchers Program (TMR).

CM991053M